Available online at sjuoz.uoz.edu.krd

Science Journal of University of Zakho

Vol. 12, No.4 pp.505–512 October-December,2024

journals.uoz.edu.krd

p-ISSN: 2663-628X
e-ISSN: 2663-6298

GREEN SYNTHESIS OF MANGANESE OXIDE NPS USING *MICROTRICHIA PEROTITII* DC PLANT EXTRACT: CHARACTERIZATION AND ANTIBACTERIAL ACTIVITY

Mercy O. Bamigboye[1*], Friday Danjuma[1]

[1]Department of Industrial Chemistry, Faculty of Physical Sciences, University of Ilorin, Ilorin 1515, Nigeria.

*Corresponding author: obaleye.mo@unilorin.edu.ng

Received: 4 Sep 2024 / Accepted: 1 Nov., 2024 / Published: 24 Nov., 2024. https://doi.org/10.25271/sjuoz.2024.12.3.1384

ABSTRACT:

This study presents a green approach to synthesizing manganese oxide nanoparticles (NPs) utilizing Microtrichia perotitii DC plant leaf extracts as a chelating agent and manganese oxide (MnO_2) as a precursor. The NPs underwent comprehensive characterization through UV-visible spectroscopy, X-ray diffraction (XRD), Fourier transform infrared spectroscopy, scanning electron microscopy, and thermogravimetric analysis. X-ray diffraction patterns indicated the synthesis of MnO NPs with an average crystallite size of 10.12 nm. Scanning electron microscope images depicted a needle-like shape with uniform distribution. Fourier transform infrared spectrophotometer analysis identified the strongest bond at 862.025 cm^{-1} corresponding to the stretching vibration mode of Mn-O NPs. Thermogravimetric analysis confirmed the thermal stability of the NPs. Furthermore, the synthesized NPs exhibited antimicrobial activity against B. Subtilis with a zone of inhibition measuring 25.625±3.01 mm.

KEYWORDS: Green synthesis, Manganese Oxide, NPs, Precursor, Spectroscopy.

1. INTRODUCTION

Nanotechnology is gaining traction because nanoparticles (NPs) and nanometric materials have unique features that allow them to be used in a variety of applications (Folorunso, 2019; Akintelu *et al.*, 2019). NPs are extremely minuscule in size. Their surface area to volume ratio causes significant differences in their properties, including biological, catalytic activity, mechanical properties, melting point, optical absorption, thermal and electrical conductivity (Shah *et al.*, 2015). These nanoscale properties make NPs valuable in fields like biomedicine, where they are used for drug delivery, diagnostics, and therapeutic applications (Khan *et al.*, 2020a).

Many biomedical researchers are drawn to metal-based NPs because they are simple to make and control, and they have different functional groups that allow them to easily associate with medications of interest, ligands, and antibodies. Metal oxide NPs have been studied for their biological applications, including antibacterial, antimycotic, antibiofilm, antioxidant, and anticancer properties (Abbasi *et al.*, 2019; Al-Radadi, 2019; Haq *et al.*, 2020; Khan *et al.*, 2020a; Khan and Lee, 2020b).

Nanomaterials generated using traditional techniques have numerous advantages and disadvantages, depending on the application (Muthukumaran *et al*., 2020; Rathinabala *et al*., 2022; Hariharan *et al*., 2020). Mechanical and chemical production of nanomaterials is often expensive, time-consuming, and possibly dangerous to the environment (Koteeswari *et al.*, 2022).

To address these challenges, researchers are increasingly exploring cost-effective and environmentally friendly NP synthesis procedures that reduce or eliminate toxic chemical reactions and prevent the formation of redundant and dangerous byproducts. This method has garnered significant attention, particularly in small-scale production units focused on sustainability (Han *et al*., 2018; Sun *et al.*, 2020).

Herbal plants and extracts have a variety of medical qualities that have been exploited to produce novel medications (Situmorang *et al.*, 2024). Plant phytochemicals, such as alkaloids, polyphenols, flavonoids, and terpenoids, have emerged as effective reducing agents for metal ion reduction during nanoparticle synthesis (Elbagory *et al.*, 2019; Gharehyakheh *et al.*, 2020). Thus, biogenic synthesis with plant leaf extract improves nanoparticle biocompatibility and accounts for the synergetic effect (Khan and Lee, 2020a).

In this regard, leaves extract of *microtrichia perotitii* DC, a species of family Asteraceae (Compositeae), was used for bioconversion of manganese ions to NPs. *Microtrichia perotitii* DC is naturally available in several countries in west Africa, including Nigeria, Senegal, Mali, Port of Guinea, Sierra Leone, Ivory Coast, and Ghana (Abdullahi, 2011). Reports demonstrated that the whole leaves extract of *Microtrichia perotitii* DC is a rich source of several biogenic phytomolecules, including alkaloids, flavonoids, tannins, phenolic compounds, saponins, and triterpenoids with various biological applications (Abdullahi, 2011).

Up to now, many plants have been utilized for the biogenic synthesis of MnO_2 NPs, *Viola betonicifolia* has been used to synthesis manganese oxide nanoparticle for its antioxidant, antifungal, antimicrobial, cytotoxicity activities and characterized with different spectroscopic techniques (Lu *et al.*, 2021) The results demonstrated that the synthesized NPs presented excellent antibacterial, and antifungal activity, against all the tested microbial species. Geetanjali et al., (2020) reported the Green Route Synthesis of Manganese Oxide NPs by Using Methanolic Extract of *Sapindus mukorossi*. It was characterized with different spectroscopic techniques (FTIR, UV-Vis, SEM, HRTEM, XRD, TGA and DLS). The synthesized manganese oxide NPs were screened for antibacterial activities on gram-positive bacteria and gram-negative bacteria. The results of the antibacterial study suggest that the manganese oxide NPs can be useful for effective growth inhibitors in microorganisms.

* Corresponding author

In this context, to the best of our knowledge, there is no information on the use of *Microtrichia perotitii* DC. This is the first study on the biogenic production of MnO_2 NPs utilizing *Microtrichia perotitii* DC extract. Thus, the current study attempted to synthesize MnO_2 NPs utilizing the plant extract of *Microtrichia perotitii* DC and evaluate their antibacterial activity.

2. MATERIALS AND METHODS

Preparation of *Microtrichia perotitii* DC plant extract

The *Microtrichia perotitii* DC used in this investigation was cleaned with sterile distilled water to remove any debris. The *Microtrichia perotitii* DC plant was air-dried for a week. The *Microtrichia perotitii* DC leaves were pulverized with a pestle and mortar. The leaves (20 g) were combined with 100 mL of distilled water and ethanol and were kept at room temperature for 24 hours (Ezhilarasi *et al.*, 2016) (the choice of water and ethanol is due to their polarity, low toxicity, high solubility of bioactive compounds and their synergistic effect to break down plant cell walls and membranes, improving the overall yield of extracted compounds.) Following the incubation period, the resultant infusion was carefully filtered using Whatmann No.1 filter paper and tested for antibacterial activity.

Preparation of Manganese oxide NPs using *Microtrichia perotitii* DC plant extract by conventional Method

Manganese oxide (MnO_2) was employed as a precursor. MnO_2 (80 mL, 0.1 M) is measured and carefully mixed with 10 ml of the plant extract, *Microtrichia perotitii* DC, drop wise with constant stirring. The mixture is then placed on the heating mantle with a magnetic stirrer for 2 hours at 80 degrees Celsius. After boiling for two hours, the mixture was allowed to cool and settle. The colloidal settling was then filtered using Whatmann no.1 filter paper and dried with a desiccator.

Antibacterial activities

Bacterial strains and Antibacterial Assay to assess the antibacterial activity of MnO NPs against six bacterial strains The disc diffusion method (Kazmi et al., 2022; Mohammed et al., 2019; Ahmed et al., 2019) was used with minor modifications for two Gram-positive strains (Staphylococcus aureus ATCC 33863, Bacillus subtilis ATCC 23857) and four Gram-negative strains (Pseudomonas aeruginosa ATCC 27853, Salmonella typhi ATCC 19430, Escherichia coli ATCC 25922, and Clostridium botulinum ATCC 19397). The bacterial strains listed above were purchased from the University of Ilorin Teaching Hospital Laboratory. The surface of nutrient agar media plates was swabbed slowly in three separate directions with an aliquot of 100 µL of inoculum that had been pre-adjusted (10^8 cells/mL) for seeding density. The plates' surface was covered with sterile filter paper discs containing 5 µL (20 mg/mL DMSO) of MnO NPs solution. The use of DMSO-infused discs as a negative control was contrasted with the use of ciprofloxacin (5 µg) loaded discs as a positive control. These was followed by an incubation period of 24 h at 37°C. After which the zone of inhibition (ZOI) was measured.

Characterization

The infrared spectrum of the solid MnO NPs was recorded by FTIR spectrometer (ZN- FTIR 530) to identify the functional Groups present in the NPs. UV-Vis spectral analysis was done by using UV-Vis spectrophotometer (SPECORD-200). The particle shape of MnO NPs was determined by SEM. The model used is Phenom Prox model. XRD (Rigaku MiniFle 600 XRD Diffractometer) was used to determine the crystallographic structures of the NPs and TG analyzer (TGA-Q500 series, TA instruments) was used to determine the thermal stability of the NPs.

Powder XRD analysis has been carried out to examine the crystallinity and to check the purity of the synthesized Nps. The optical properties of the nanoparticle were analyzed using UV-Vis spectroscopy. The presence of functional group was analyzed by FTIR spectroscopy. The thermal stability of the synthesized nanoparticle was analyzed by TGA. Morphology of the synthesized manganese dioxide NPs were analyzed using SEM.

Statistical Analysis

The data obtained from the experiment was utilized for statistical analysis. All trials were conducted in triplicate, and the findings are given as mean ± standard deviation. To ascertain the statistical significance, we used SPSS with a predetermined significance level (at $p < 0.05$).

3. RESULTS AND DISCUSSION

Fourier transforms infrared spectroscopy (FTIR) studies

FTIR spectroscopy was used to identify functional groups present on the synthesized MnO2 NPs, as shown in Figure 1. The analysis was conducted using the KBr pellet technique in the spectral range of 4000–400 cm^{-1} to confirm the purity and composition of the NPs. The bands observed between 615 and 862 cm^{-1} are assigned to the stretching vibrations of the O−Mn−O bond, indicating the presence of manganese oxide in the sample (Jaganyi *et al.*, 2013; Yang *et al.*, 2004; Yang *et al.*, 2005) The distinct signal at 862 cm^{-1} is attributed to Mn-O stretching, corroborating the formation of manganese oxide NPs and is similar to the Mn-O stretching frequency obtained by (Kumar *et al.*, 2017). A significant peak at 3343 cm^{-1} corresponds to O-H stretching, likely from hydroxyl groups in the plant extract, which play a crucial role in the reduction and stabilization of NPs (Iravani, 2011). This suggests that the phytochemicals in the plant not only assist in NPs formation but also enhance their stability. The peak at 1679 cm^{-1} is attributed to C=O stretching vibrations, signifying the presence of carboxylic groups, which are involved in capping the NPs and enhancing their stability forming strong interactions with the nanoparticle surface (Ahmed *et al.*, 2016). A band at 1068 cm^{-1} is associated with C-O stretching further confirming the involvement of organic compounds from the plant, while the peak at 2886 cm^{-1} is linked to C-H stretching of alkenes, confirming the involvement of organic compounds from the plant extract in the synthesis process (Pooja *et al.*, 2022). Additionally, the band at 1383 cm^{-1} corresponds to C-N stretching vibrations, indicative of amine groups, which further contribute to nanoparticle stability as well as coating or capping of NPs (Anuradha *et al.*, 2014; Abbasi *et al.*, 2014). The FTIR analysis confirms the successful synthesis of MnO Nps with the various functional groups from the plant extract aiding the reduction, capping and stabilization of the NPs, these metal-oxygen vibrational frequencies align with previous literature, confirming the successful synthesis of MnO2 NPs (Kumar *et al.*, 2017).

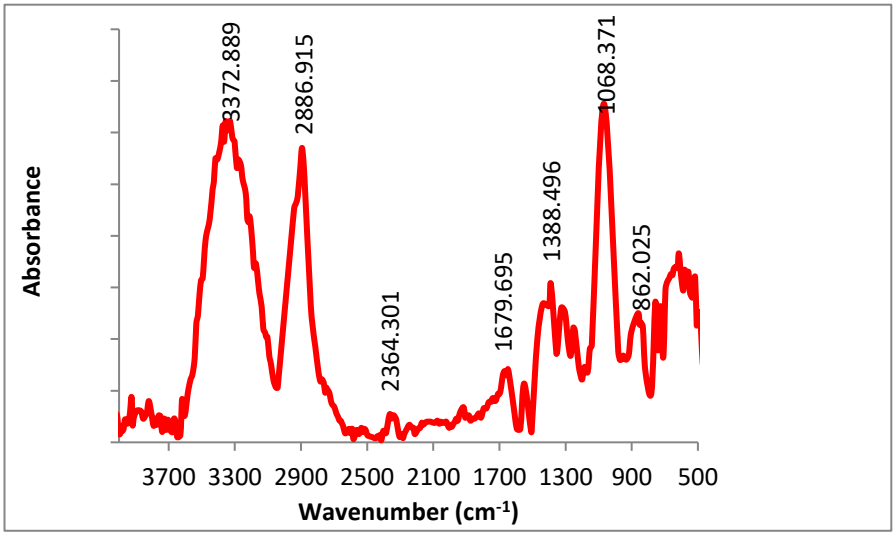

Figure 1: FTIR spectrum of *M. perotitii* synthesized MnO NPs

Optical properties of MnO NPs

UV-visible absorption study is one of the most convenient techniques for characterizing NPs and thus provides information about the optical properties of NPs (Luo, 2007). Absorption spectrum Figure 2 shows MnO NPs characterized from ultraviolet (UV) to visible (250-700 nm). NPs absorb light in the UV-visible region (Kumar *et al.*, 2009). The UV-Visible absorption intensity of NPs normally increases as their concentration increases (Kumar *et al.*, 2013). In the current investigation, MnO NPs exhibited a distinct absorption peak at approximately 340 nm which indicated the formation of MnO_2 NPs (Joshi *et al.*, 2020). As the wavelength increased, the absorbance intensity decreased, showing that formation did not occur at a long wavelength. Previous research by (Manjula *et al.*, 2019) revealed that MnO NPs have an absorption peak in that wavelength region, which supports the current study.

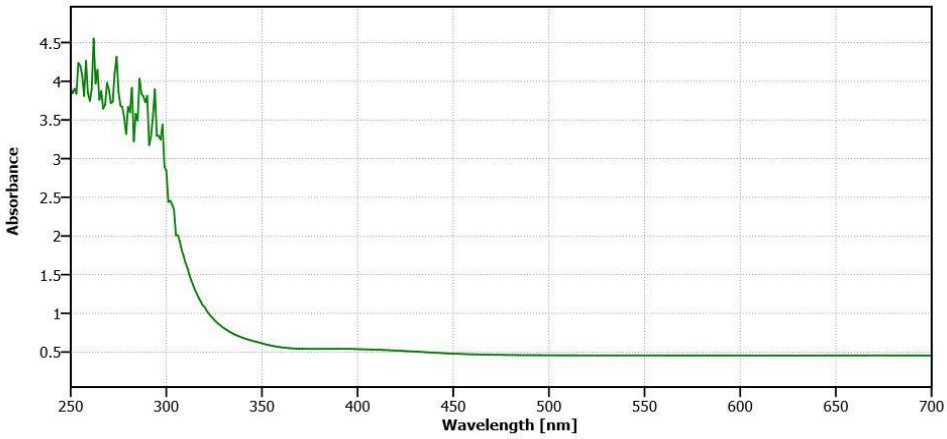

Figure 2: Absorption spectrum of *M. perotitii* synthesized MnO NPs

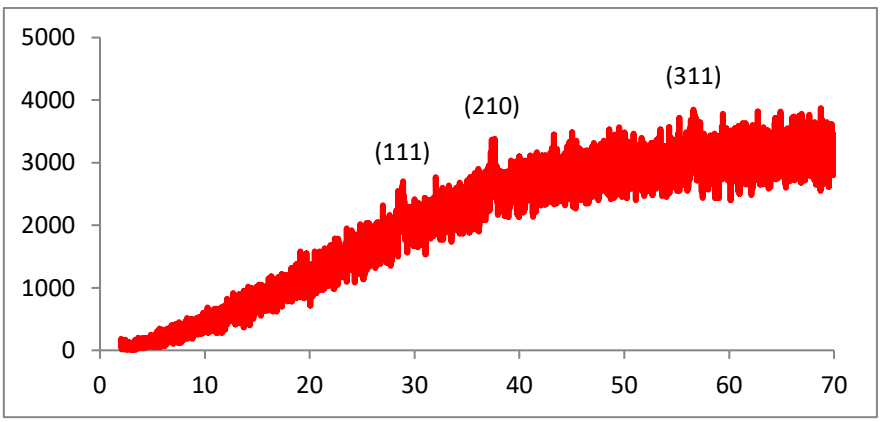

Figure 3: XRD pattern of *M. perotitii* synthesized MnONPs

X-ray diffractometry (XRD) analysis

The phase and purity of the products are examined by X-ray diffraction (XRD). From the XRD pattern, it can be seen that manganese dioxide metal NPs synthesized is crystalline with low intensity. Figure 3 shows the XRD patterns for the produced MnO NPs. The presence of MnO causes diffraction peaks at 2θ = 28.83°, 37.3°, and 56.67°, corresponding to the (111), (210), and (311) crystal planes (JCPDS file no. 00-001-0799). The crystallite size of MnO nanocrystals was calculated using Debye Scherer's equation:

$$D = \frac{0.89\lambda}{\beta \times \cos\theta} \quad (1)$$

Where D is the average crystal size, λ is the X-ray wavelength, and β is the full width at half maximum (FWHM). The detected peaks suggested that the particles were face-centered cubic, with an average crystallite size of 10.12 nm which is similar to the results obtained by (Geetanjali *et al.*, 2024). The produced MnO_2 NPs obtained have poor crystalline properties (Manjula *et al.*, 2019). Metal oxide NPs' crystallinity can be affected by their size, shape, and the reagents used during synthesis, hence the different peaks. (Lefojane *et al.*, 2020)

Surface morphology characterization

SEM was used to study the morphology and surface structure of produced MnO NPs. SEM micrographs show the overall look of the derived product (Sinha *et al.*, 2011). The micrograph shows that it is totally covered in a needle-like structure with uniform distribution, implying some level of nanoparticle aggregation which may be used due to the influence of the synthesis method. The SEM image of prepared MnO_2 NPs was supported with the previously published data by (Prasad & Patra, 2017a). It is well acknowledged that surface morphology has an important impact on the performance of nanostructure materials (Geetanjali *et al*., 2024). Therefore, the SEM micrograph in Figure 4 demonstrates that the homogenous disparity, shape, and size of these particles can play an important role in their varied roles.

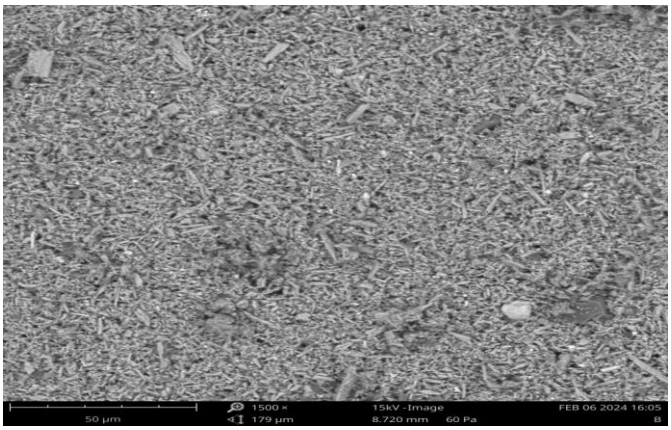

Figure 4: SEM micrograph *M. perotitii* synthesized MnO NPs

Thermogravimetric Analysis (TGA).

Thermogravimetric analysis was performed on *Microtrichia perotitii* DC plant extracts to investigate the heat stability and degradation pattern of the NPs generated. The TGA spectra of MnO NPs demonstrate that the sample decomposes significantly at higher temperatures. The data reveals that when the temperature rises from 25 to 100 °C, the weight % of the NPs decreases, which is due to the disintegration of water molecules and ethanol on the NPs' surfaces (Srivastava *et al.*, 2021). As seen in Figure 5, increasing the temperature to 300-450 °C results in a significant 70-75% weight loss, most likely due to the numerous volatile components present in the plant sample. No additional weight loss was seen when the temperature was raised from around 450 °C to 900 °C; these findings indicate the stability of MnO NPs in that temperature range. As a result, the thermogram clearly reveals that MnO NPs are thermally stable at temperatures up to 900 degrees Celsius.

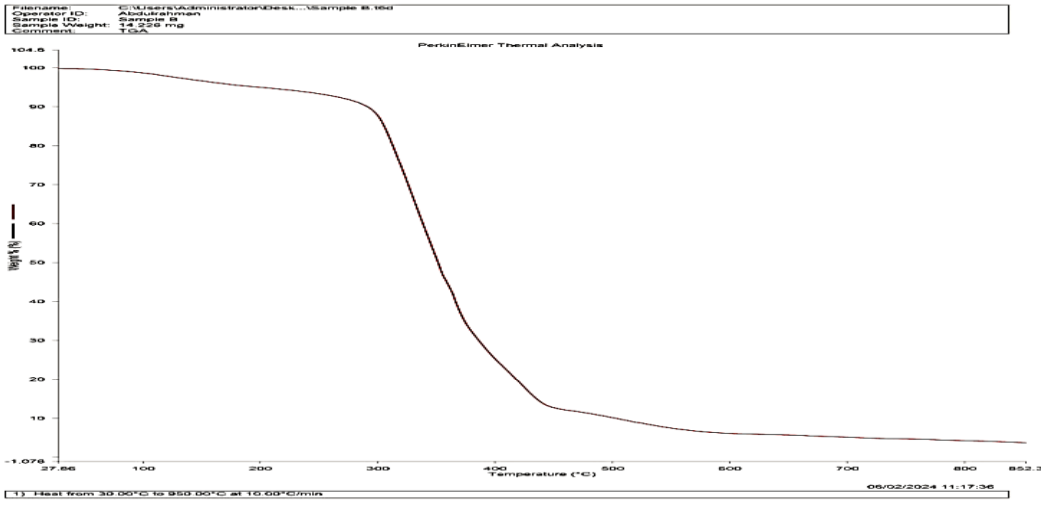

Figure 5: TGA curve of *M. perotitii* synthesized MnO NPs

Evaluation of antibacterial activity using MnO NPs prepared using *Microtrichia perotitii* DC plant extract

Green MnO_2 NPs demonstrated strong broad-spectrum antibacterial activity against all tested bacterial pathogens. The ratios of phytochemical components, such as polyphenols and flavonoids in the plant extract, directly influence the antimicrobial properties of the plant (Hussain *et al.,* 2023). The relative antibacterial activity of MnO NPs prepared from *Microtrichia perotitii* DC plant extract was tested against bacterial pathogens including *Staphylococcus aureus* (+), *Bacillus subtilis* (+), *Pseudomonas aeruginosa* (-), *Salmonella typhi* (-), *Escherichia coli* (-), and *Clostridium botulinum* (-) and it was found out that MnO_2 NPs achieved the maximum zone of inhibition (ZI) estimated as mentioned in Table 1. This had antibacterial activity against the test organisms as compared to positive control. The obtained MnO nanoparticle was efficient against Gram-positive *B. subtilis* (25.625±3.01) and *S. aureus* (23.62±2.52), with a greater zone of inhibition than Gram negative bacterial pathogens, as indicated in Table 1 and Figure 2. The findings are comparable with those of Helen and Rani (2015). This difference in efficacy can be attributed to structural variations in bacterial cell walls**,** Gram-positive bacteria have a thick peptidoglycan layer whereas Gram-negative bacteria have thin cell walls (Mai-prochnow, 2016). Though Gram-positive bacteria have thicker cell walls than Gram-negative bacteria, antibiotics can easily get access to the peptidoglycan. This is however not feasible for Gram-negative bacteria because unlike Gram-positive bacteria, Gram-negative bacteria have an outer membrane which serves as a protective layer and is essential for survival. Gram-negatives have been identified to be more inclined to antibiotic resistance (Allen et al., 2010; Romaniuk and Cegelski, 2015; Heesterbeek *et al*., 2019) and hence result in the evolution of many 'resistant-related' infections (Davies and Davies, 2010). Several studies have also indicated that MnO NPs generated from plant extract have strong antibacterial action, which supports the current investigation's findings (Jayandran *et al.*, 2015; Haneefa *et al*., 2017a; Haneefa *et al.,* 2017b).

Table 1: Antimicrobial activity of *M. perotitii* synthesized MnO NPs

Test organisms	**Activity of MnO NPs (mm)**	**Ciprofloxacin (5 µg disc)**
S. aureus	23.625 ± 2.52^{e}	25.06 ± 3.26^{d}
P. aeruginosa	19.100 ± 2.01^{d}	21.55 ± 1.50^{c}
S. tyhi	10.775 ± 0.83^{b}	18.55 ± 2.30^{a}
E. coli	0.000 ± 0.00^{a}	20.70 ± 3.57^{c}
C. botulinum	15.600 ± 1.27^{c}	19.55 ± 0.79^{f}
B. subtilis	25.625 ± 3.01^{f}	21.38 ± 2.10^{d}

The superscript lettered (a-f) indicate significant difference (at $p < 0.05$) when subject to SPSS test. The findings are given as mean ± standard deviation

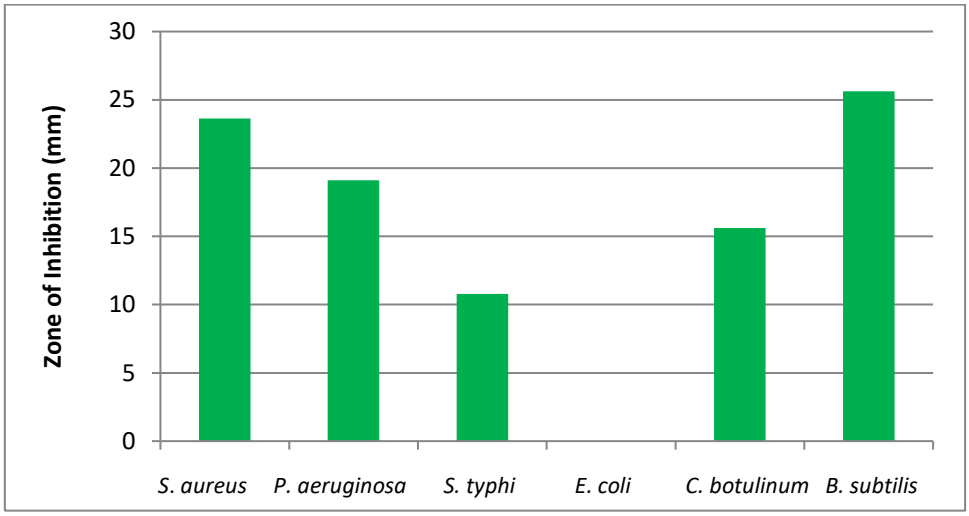

Figure 6: Antimicrobial activity of *M. perotitii* synthesized MnO NPs

CONCLUSION

The current study describes a green synthesis of MnO NPs that is both cost-effective and environmentally friendly, using *Microtrichia perotitii* DC plant extracts as reducing and capping agents. UV-Vis spectroscopy, FTIR, SEM, XRD, and TGA were utilized to investigate the MnO NPs. The UV-Vis spectrum revealed an absorption band at 340 nm from MnO NPs. The FTIR analysis revealed that metal oxide NPs were reduced from zinc ion solutions to MnO NPs with a stretching vibration of 862 cm^{-1}. SEM micrographs revealed the needle-like structure of MnO NPs. XRD analysis reveals MnO NPs' low crystallinity, with an estimated crystallite size of 10.12 nm. The synthesized manganese oxide NPs showed excellent antibacterial activity against Gram-positive more than Gram-negative bacterial strains. The study is a primary step towards the application of manganese oxide NPs in the biomedical field.

REFERENCES

Abbasi, B. A., Iqbal, J., Mahmood, T., Ahmad, R., Kanwal, S., & Afridi, S. (2019). Plant-mediated synthesis of nickel oxide Nanoparticles (NiO) via Geranium wallichianum: characterization and different biological applications. *Materials Research Express*, *6*(8), 0850a7. https://doi.org/10.1088/2053-1591/ab23e1

Abbasi, T., Anuradha, J., Ganaie, S., & Abbasi, S. (2014). Gainful utilization of the highly intransigent weed

ipomoea in the synthesis of gold Nanoparticles. *Journal of King Saud University - Science*, *27*(1), 15–22. https://doi.org/10.1016/j.jksus.2014.04.001

Abdullahi, M. (2011). Phytochemical Screening and Biological Studies of the Leaves of Microtrichia perotitii DC (Asteraceae). *European Journal of Medicinal Plants*, *1*(3), 88–97. https://doi.org/10.9734/ejmp/2011/188

Ahmed, M., Qadir, M. A., Shafiq, M. I., Muddassar, M., Samra, Z. Q., & Hameed, A. (2016). Synthesis, characterization, biological activities and molecular modeling of Schiff bases of benzene sulfonamides bearing curcumin scaffold. *Arabian Journal of Chemistry*, *12*(1), 41–53. https://doi.org/10.1016/j.arabjc.2016.11.017

Ahmed, S., Saifullah, N., Ahmad, M., Swami, B. L., & Ikram, S. (2015). Green synthesis of silver Nanoparticles using Azadirachta indica aqueous leaf extract. *Journal of Radiation Research and Applied Sciences*, *9*(1), 1–7. https://doi.org/10.1016/j.jrras.2015.06.006

Akintelu, S. A., Folorunso, A. S., & Ademosun, O. T. (2019). Instrumental characterization and antibacterial investigation of silver Nanoparticles synthesized from garcinia kola leaf. *Journal of Drug Delivery and Therapeutics*, *9*(6-s), 58–64. https://doi.org/10.22270/jddt.v9i6-s.3749

Allen, H. K., Donato, J., Wang, H. H., Cloud-Hansen, K. A., Davies, J., & Handelsman, J. (2010). Call of the wild: antibiotic resistance genes in natural environments. *Nature Reviews Microbiology*, *8*(4), 251–259. https://doi.org/10.1038/nrmicro2312

Al-Radadi, N. S. (2018). Green synthesis of platinum Nanoparticles using Saudi's Dates extract and their usage on the cancer cell treatment. *Arabian Journal of Chemistry*, *12*(3), 330–349. https://doi.org/10.1016/j.arabjc.2018.05.008

Anuradha, J., Abbasi, T., & Abbasi, S. (2014). An eco-friendly method of synthesizing gold Nanoparticles using an otherwise worthless weed pistia (Pistia stratiotes L.). *Journal of Advanced Research*, *6*(5), 711–720. https://doi.org/10.1016/j.jare.2014.03.006

Davies, J., & Davies, D. (2010). Origins and evolution of antibiotic resistance. *Microbiology and Molecular Biology Reviews*, *74*(3), 417–433. https://doi.org/10.1128/mmbr.00016-10

Elbagory, A. M., Hussein, A. A., & Meyer, M. (2019). The In Vitro Immunomodulatory Effects Of Gold Nanoparticles Synthesized From Hypoxis hemerocallidea Aqueous Extract And Hypoxoside On Macrophage And Natural Killer Cells *International Journal of Nanomedicine*, *Volume 14*, 9007–9018. https://doi.org/10.2147/ijn.s216972

Ezhilarasi, A. A., Vijaya, J. J., Kaviyarasu, K., Maaza, M., Ayeshamariam, A., & Kennedy, L. J. (2016). Green synthesis of NiO Nanoparticles using Moringa oleifera extract and their biomedical applications: Cytotoxicity effect of NPs against HT-29 cancer cells. *Journal of Photochemistry and Photobiology B Biology*, *164*, 352–360. https://doi.org/10.1016/j.jphotobiol.2016.10.003

Folorunso, A., Akintelu, S., Oyebamiji, A. K., Ajayi, S., Abiola, B., Abdusalam, I., & Morakinyo, A. (2019). Biosynthesis, characterization and antimicrobial activity of gold Nanoparticles from leaf extracts of Annona muricata. *Journal of Nanostructure in Chemistry*, *9*(2), 111–117. https://doi.org/10.1007/s40097-019-0301-1

Geetanjali., Tamta A., Chandra B., Kandpal N. D., Joshi R., Green Route Synthesis of Manganese Oxide Nanoparticles by Using Methanolic Extract of Sapindus mukorossi (reetha). Journal of Water Environment and Nanotechnology, 2024; 9(2): 211-222. https://doi.org/10.22090/jwent.2024.02.07

Gharehyakheh, S., Ahmeda, A., Haddadi, A., Jamshidi, M., Nowrozi, M., Zangeneh, M. M., & Zangeneh, A. (2020). Effect of gold Nanoparticles synthesized using the aqueous extract of Satureja hortensis leaf on enhancing the shelf life and removing Escherichia coli O157:H7 and Listeria monocytogenes in minced camel's meat: The role of nanotechnology in the food industry. *Applied Organometallic Chemistry*, *34*(4). https://doi.org/10.1002/aoc.5492

Han, K., Huang, H., Gong, Q., Si, T., Zhang, Z., & Zhou, G. (2018). Temperature-induced hierarchical Tremella-like and Pinecone-like NiO microspheres for high-performance supercapacitor electrode materials. *Journal of Materials Science*, *53*(17), 12477–12491. https://doi.org/10.1007/s10853-018-2532-9

Haneefa, M.M. (2017). Green Synthesis Characterization and Antimicrobial Activity Evaluation of Manganese Oxide Nanoparticles and Comparative Studies with Salicylalchitosan Functionalized Nanoform. *Asian Journal of Pharmaceutics*, *11*. https://doi.org/10.22377/AJP.V11I01.1045

Haneefa, M. M., M, J., & V, B. (2017a). Evaluation of antimicrobial activity of green-synthesized manganese oxide Nanoparticles and comparative studies with curcumininaniline functionalized nanoform. *Asian Journal of Pharmaceutical and Clinical Research*, *10*(3), 347. https://doi.org/10.22159/ajpcr.2017.v10i3.16246

Haq, S., Rehman, W., Waseem, M., Shah, A., Khan, A. R., Rehman, M. U., Ahmad, P., Khan, B., & Ali, G. (2020). Green synthesis and characterization of tin dioxide Nanoparticles for photocatalytic and antimicrobial studies. *Materials Research Express*, *7*(2), 025012. https://doi.org/10.1088/2053-1591/ab6fa1

Hariharan, D., Thangamuniyandi, P., Christy, A. J., Vasantharaja, R., Selvakumar, P., Sagadevan, S., Pugazhendhi, A., & Nehru, L. (2019a). Enhanced photocatalysis and anticancer activity of green hydrothermal synthesized Ag@TiO2 Nanoparticles. *Journal of Photochemistry and Photobiology B Biology*, *202*, 111636. https://doi.org/10.1016/j.jphotobiol.2019.111636

Heesterbeek, D. a. C., Martin, N. I., Velthuizen, A., Duijst, M., Ruyken, M., Wubbolts, R., Rooijakkers, S. H. M., & Bardoel, B. W. (2019). Publisher Correction: Complement-dependent outer membrane perturbation sensitizes Gram-negative bacteria to Gram-positive specific antibiotics. *Scientific Reports*, *9*(1). https://doi.org/10.1038/s41598-019-43208-4

Helen, S., Hebzi, M., & Rani, E. (2015). Characterization and Antimicrobial Study of Nickel Nanoparticles Synthesized from Dioscorea (Elephant Yam) by Green Route. *International Journal of Science and Research (IJSR)*, *4*(11), 216–219. https://doi.org/10.21275/v4i11.nov151105

Hussain, S., Muazzam, M. A., Ahmed, M., Ahmad, M., Mustafa, Z., Murtaza, S., Ali, J., Ibrar, M., Shahid, M., & Imran, M. (2023). Green synthesis of nickel oxide Nanoparticles using Acacia nilotica leaf extracts and investigation of their electrochemical and biological properties. *Journal of Taibah University for Science*, *17*(1). https://doi.org/10.1080/16583655.2023.2170162

Iravani, S. (2011). Green synthesis of metal Nanoparticles using plants. *Green Chemistry*, *13*(10), 2638. https://doi.org/10.1039/c1gc15386b

Jaganyi, D., Altaf, M., & Wekesa, I. (2012). Synthesis and characterization of whisker-shaped MnO2 nanostructure at room temperature. *Applied Nanoscience*, *3*(4), 329–333. https://doi.org/10.1007/s13204-012-0135-3

Jayandran, M., Haneefa, M., & Balasubramanian, V. (2015). Green synthesis and characterization of Manganese Nanoparticles using natural plant extracts and its evaluation of antimicrobial activity. *Journal of Applied Pharmaceutical Science*, 105–110. https://doi.org/10.7324/japs.2015.501218

Joshi, N. C., Joshi, E., & Singh, A. (2020). Biological Synthesis, Characterisations and Antimicrobial activities of manganese dioxide (MnO_2) Nanoparticles. *Research Journal of Pharmacy and Technology*, *13*(1), 135. https://doi.org/10.5958/0974-360x.2020.00027.x

Kazmi, S. T. B., Naz, I., Zahra, S. S., Nasar, H., Fatima, H., Farooq, A. S., & Haq, I. (2022). Phytochemical analysis and comprehensive evaluation of pharmacological potential of Artemisia brevifolia Wall. ex DC. *Saudi Pharmaceutical Journal*, *30*(6), 793–814. https://doi.org/10.1016/j.jsps.2022.03.012

Khan, S. A., & Lee, C. (2020a). Green biological synthesis of Nanoparticles and their biomedical applications. In *Nanotechnology in the life sciences* (pp. 247–280). https://doi.org/10.1007/978-3-030-44176-0_10

Khan, S. A., & Lee, C. (2020b). Recent progress and strategies to develop antimicrobial contact lenses and lens cases for different types of microbial keratitis. *Acta Biomaterialia*, *113*, 101–118. https://doi.org/10.1016/j.actbio.2020.06.039

Koteeswari, P., Sagadevan, S., Fatimah, I., Sibhatu, A. K., Razak, S. I. A., Soga, T., & Léonard, E. (2022). Green synthesis and characterization of copper oxide Nanoparticles and their photocatalytic activity. *Inorganic Chemistry Communications*, *144*, 109851. https://doi.org/10.1016/j.inoche.2022.109851

Kumar, V., & Yadav, S. K. (2008). Plant-mediated synthesis of silver and gold Nanoparticles and their applications. *Journal of Chemical Technology & Biotechnology*, *84*(2), 151–157. https://doi.org/10.1002/jctb.2023

Kumar, V., and Yadav, S.K. (2013). Influence of physiochemical factors on size of gold Nanoparticles synthesised using leaf extract of Syzygium cumini L. *Journal of Chemical Science and Technol*ogy. 2, 104–113.

Kumar, V., Singh, K., Panwar, S., & Mehta, S. K. (2017). Green synthesis of manganese oxide Nanoparticles for the electrochemical sensing of p-nitrophenol. *International Nano Letters.*, *7*(2), 123–131. https://doi.org/10.1007/s40089-017-0205-3

Lefojane, R., Direko, P., Mfengwana, P., Mashele, S., Matinise, N., Maaza, M., & Sekhoacha, M. (2020). Green Synthesis of Nickel Oxide (NiO) Nanoparticles Using Spirostachys africana Bark Extract. *Asian Journal of Scientific Research*, *13*(4), 284–291. https://doi.org/10.3923/ajsr.2020.284.291

Lu, H., Zhang, X., Khan, S. A., Li, W., & Wan, L. (2021). Biogenic Synthesis of MnO2 Nanoparticles With Leaf Extract of Viola betonicifolia for Enhanced Antioxidant, Antimicrobial, Cytotoxic, and Biocompatible Applications. *Frontiers in Microbiology*, *12*. https://doi.org/10.3389/fmicb.2021.761084

Luo, Y. (2006). Preparation of MnO_2 Nanoparticles by directly mixing potassium permanganate and polyelectrolyte aqueous solutions. *Materials Letters*, *61*(8–9), 1893–1895. https://doi.org/10.1016/j.matlet.2006.07.165

Mai-Prochnow, A., Clauson, M., Hong, J., & Murphy, A. B. (2016). Gram positive and Gram negative bacteria differ in their sensitivity to cold plasma. *Scientific Reports*, *6*(1). https://doi.org/10.1038/srep38610

Manjula, R., Thenmozhi, M., Thilagavathi, S., Srinivasan, R., & Kathirvel, A. (2019). Green synthesis and characterization of manganese oxide Nanoparticles from Gardenia resinifera leaves. *Materials Today Proceedings*, *26*, 3559–3563. https://doi.org/10.1016/j.matpr.2019.07.396

Mohammed, I. A., Ahmed, M., Ikram, R., Muddassar, M., Qadir, M. A., & Awang, K. B. (2018). Synthesis of 1,3-benzoxazines based on 2,4,4-trimethyl-7,2',4'-trihydroxy flavan: antibacterial, anti-inflammatory, cyclooxygenase-2 inhibition and molecular modelling studies. *Letters in Drug Design & Discovery*, *16*(1), 58–65. https://doi.org/10.2174/1570180815666180420100922

Muthukumaran, M., Dhinagaran, G., Venkatachalam, K., Sagadevan, S., Gunasekaran, S., Podder, J., Mohammad, F., Shahid, M., & Oh, W. C. (2020). Green synthesis of cuprous oxide Nanoparticles for environmental remediation and enhanced visible-light photocatalytic activity. *Optik*, *214*, 164849. https://doi.org/10.1016/j.ijleo.2020.164849

Pooja R, Varsha S L, Aliya M S, Chetana Kumar T, Damini B M, Divya H K, Lakshmi J, Sushma J M, Swati K, Annapurneshwari M H, Ravi M, & Vedamurthy A B. (2022). Phytochemical screening, GCMS, UV-vis and FTIR analysis of leaf methanolic extract of Sapindus mukorossi L. *International Journal of Progressive Research in Science and Engineering*, *3*(05), 97–104.

Prasad, K. S., & Patra, A. (2017a). Green synthesis of MnO2 nanorods using Phyllanthus amarus plant extract and their fluorescence studies. *Green Processing and Synthesis*, *6*(6). https://doi.org/10.1515/gps-2016-0166

Rathinabala, R., Thamizselvi, R., Padmanabhan, D., Alshahateet, S. F., Fatimah, I., Sibhatu, A. K., Weldegebrieal, G. K., Razak, S. I. A., & Sagadevan, S. (2022). Sun light-assisted enhanced photocatalytic activity and cytotoxicity of green synthesized SnO2 NPs. *Inorganic Chemistry Communications*, *143*, 109783. https://doi.org/10.1016/j.inoche.2022.109783

Romaniuk, J. A. H., & Cegelski, L. (2015). Bacterial cell wall composition and the influence of antibiotics by cell-wall and whole-cell NMR. *Philosophical Transactions of the Royal Society B Biological Sciences*, *370*(1679), 20150024. https://doi.org/10.1098/rstb.2015.0024

Shah, M., Fawcett, D., Sharma, S., Tripathy, S. K., & Poinern, G. E. J. (2015). Green synthesis of metallic Nanoparticles via biological entities. *Materials*, *8*(11), 7278–7308. https://doi.org/10.3390/ma8115377

Sinha, A., Singh, V. N., Mehta, B. R., & Khare, S. K. (2011). Synthesis and characterization of monodispersed orthorhombic manganese oxide Nanoparticles produced by Bacillus sp. cells simultaneous to its bioremediation. *Journal of Hazardous Materials*, *192*(2), 620–627. https://doi.org/10.1016/j.jhazmat.2011.05.103

Situmorang, P. C., Ilyas, S., Nugraha, S. E., Syahputra, R. A., & Rahman, N. M. a. N. A. (2024). Prospects of compounds of herbal plants as anticancer agents: a comprehensive review from molecular pathways. *Frontiers in Pharmacology*, *15*. https://doi.org/10.3389/fphar.2024.1387866

Srivastava, V., Beg, M., Sharma, S., & Choubey, A. K. (2021). Application of manganese oxide Nanoparticles synthesized via green route for improved performance of water-based drilling fluids. *Applied Nanoscience*, *11*(8), 2247–2260. https://doi.org/10.1007/s13204-021-01956-8

Sun, B., Zhang, Y., Zhang, R., Yu, H., Zhou, G., Zhang, H., & Wang, J. (2017). High-Order nonlinear optical properties generated by different electron transition processes of NIO nanosheets and applications to ultrafast lasers. *Advanced Optical Materials*, *5*(8). https://doi.org/10.1002/adom.201600937

Yang, X., Makita, Y., Liu, Z., Sakane, K., & Ooi, K. (2004). Structural Characterization of Self-Assembled MnO2Nanosheets from Birnessite Manganese Oxide Single Crystals. *Chemistry of Materials*, *16*(26), 5581–5588. https://doi.org/10.1021/cm049025d

Yang, Z., Xia, G., & Stevenson, J. W. (2005). Mn[sub 1.5]Co[sub 1.5]O[sub 4] Spinel Protection Layers on Ferritic Stainless Steels for SOFC Interconnect Applications. *Electrochemical and Solid-State Letters*, *8*(3), A168. https://doi.org/10.1149/1.1854122